Helical Assemblies of One-Dimensional Supramolecular Polymers Composed of Helical Macromolecules: Generation of Circularly Polarized Light Using an Infinitesimal Chiral Source

Tomoyuki Ikai,*[,†,‡] Mitsuhiro Okubo,[†] and Yuya Wada[†]

[†]Graduate School of Natural Science and Technology, Kanazawa University, Kakuma-machi, Kanazawa 920-1192, Japan

[‡]Department of Molecular and Macromolecular Chemistry, Graduate School of Engineering, Nagoya University, Chikusa-ku, Nagoya 464-8603, Japan

ABSTRACT: We report the synthesis of one-dimensional supramolecular polymers composed of one-handed helical macromolecules bearing fluorescent pendant groups, and the generation of circularly polarized light based on hierarchical chiral amplification starting from a tiny amount of chiral substituent. Copolymerization of benzo[1,2-*b*:4,5-*b*']dithiophene-appended achiral/chiral isocyanides (99:1, mol/mol) with a solid-state photoluminescence feature afforded sub-micrometer supramolecular fibers, in which almost perfect single-handed helical polyisocyanides were noncovalently connected end-to-end. The resulting helical supramolecular polymers were further helically assembled to form a cholesteric liquid crystal film with an intense circularly polarized luminescence (CPL) signal. Surprisingly, the supramolecular system containing only 0.01 mol% of the chiral monomer unit also emitted the observable circularly polarized light owing to multiple chiral amplification from an infinitesimal point chirality to helical chirality, and then to supramolecular chirality. Furthermore, chiral information was efficiently transferred from the helically assembled supramolecular system containing 1 mol% of the chiral unit to achiral dye molecules blended in the film, allowing full-color tunable induced CPL with luminescence dissymmetry factors greater than 1.0×10^{-2}. This unprecedentedly strong chiral amplification enables the creation of helical supramolecular polymers and chirally assembled systems with various chiral functions based solely on an infinitesimal chiral source.

INTRODUCTION

The origin of homochirality in nature, particularly in biomacromolecules composed of L-amino acid- or D-sugar-based repeating units, remains largely mysterious,[1] but is closely related to chiral amplification, a phenomenon capable of creating chiral compounds with higher optical purity using a smaller chiral bias.[2] In 1989, Green et al. reported the seminal example of artificial chiral amplification in copolymerizations of achiral and chiral monomers, namely, the "sergeants and soldiers" effect,[3] in which a minor chiral component efficiently induces one-handed helicity in the resulting polymer backbones containing a large number of achiral units.[4] Using this type of chiral amplification, various helical macromolecules[5] and supramolecular systems[1b,6] with an excess handedness have been produced to date, and applied in the fields of asymmetric catalysis,[7] chiral recognition,[8] and circularly polarized luminescence (CPL).[9] A key advantage of using chiral amplification to develop chiral materials is that the use of chiral sources, which are sometimes precious and hard to obtain, can be minimized, leading to a reduction in the time/energy needed to prepare a large amount of optically active ingredients using synthetic and/or resolution techniques.

Recently, we discovered a unique one-step synthesis of one-dimensional (1-D) supramolecular polymers through a nickel-catalyzed polymerization of glycine-based isocyanides (**1A$_X$**), in which macromolecular building blocks with a helical conformation were noncovalently connected end-to-end through multiple intermolecular hydrogen bonds (Figure 1A).[10] Although the reaction mechanism, termed the "transit-type merry-go-round (MGR)" mechanism, has yet to be fully elucidated, the growth of macromolecular chains and chain transfer accompanied by the formation of supramolecular linkages have been shown to occur continuously in an alternating manner. Consequently, the direct conversion of polymerizable small molecules into 1-D macromolecular assemblies could be achieved, which is a hitherto unseen phenomenon in both nature and artificial systems. Furthermore, the copolymerization with chiral (optically active) isocyanides (**1L$_X$**) produced almost perfect one-handed helical supramolecular fibers through dual intramolecular/intermolecular chiral amplification, in which stereochemical communication between macromolecular building blocks played an indispensable role.

CPL has attracted much interest, not only for its potential to obtain information about excited-state chirality, but also for its practical applications in a variety of photonic technologies, including optical tags for security, 3D display devices, biological probes, and quantum encryption.[11] To date, various CPL-active materials, including chiral lanthanide complexes[12] and chiral π-conjugated molecules,[13] supramolecules,[14] and polymers,[5g,15] have been reported. However, CPL materials remain at an early stage of development, with further research required to understand the relationships between molecular structures/arrangements and CPL performance for the design of practical materials necessary for demanding applications. CPL is not always derived from the emission of nonracemic chiral

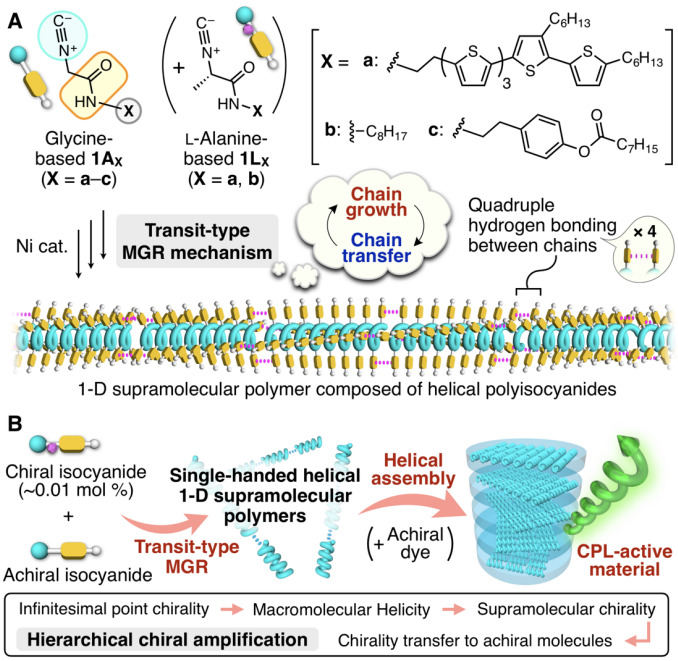

Figure 1. (A) Schematic illustration of one-step synthesis of the 1-D supramolecular polymer composed of helical polyisocyanides through (co)polymerization of amino acid-based isocyanides via the "transit-type merry-go-round (MGR)" mechanism. (B) Helical assembly of single-handed helical 1-D supramolecular polymers in the presence or absence of achiral fluorescent dye to generate circularly polarized light through hierarchical chiral amplification starting from an infinitesimal point chirality.

compounds, but can be produced by achiral and racemic compounds. In fact, Liu and co-workers reported unique CPL-active supramolecular systems comprising only an achiral molecule, the chirality of which originated from spontaneous symmetry breaking through stochastic self-assembly into left- or right-handed twisted fibers.[16] CPL induced by achiral molecules and polymers was also obtained through the supramolecular co-assembly of chiral and achiral components accompanied by chiral information transfer.[14a,b,e,f,h,17] Our group has introduced a facile approach to generating both left- and right-handed circularly polarized light from a totally racemic fluorescent molecule through conglomerate crystallization followed by random selection of the resulting single crystals.[18]

To explore untapped opportunities in functional polymers, supramolecular assemblies, and chiral amplification, in this study, we have developed CPL-active helical assemblies of 1-D supramolecular polymers comprising single-handed helical macromolecules by taking advantage of copolymerization via the "transit-type MGR" mechanism (Figure 1B). The benzo[1,2-*b*:4,5-*b*']dithiophene (BDT) unit was employed as a key structural element for pendant groups (see Figure 2A), because its inherently good fluorescence properties, both in solution and solid states, favored our desired functionalization.[19] We have shown that circularly polarized light can be produced by the supramolecular system containing an infinitesimal chiral unit (0.01 mol%). The full-color tunable induced CPL was also achieved by a combination of achiral dye molecules owing to the highly hierarchical chiral amplification from point chirality to helical chirality, and further to supramolecular chirality. This study focuses on the development of chiral functions using the supramolecular helical assembly of one-dimensional supramolecular polymers and thus is critically different from our previous work.[10]

RESULTS AND DISCUSSION

Synthesis of a 1-D Supramolecular Polymer Composed of Helical Macromolecules. The synthetic route to prepare achiral glycine-based (**3**) and chiral alanine-based (**2L** and **2D**) isocyanide monomers bearing a BDT-based π-conjugated unit as a fluorescent pendant group is shown in Scheme S1. Monomers **2L** and **2D** were purified by chiral high-performance liquid chromatography (HPLC) to ensure high optical purities of >99% ee (Figure S1A). We first investigated the homopolymerization of **3** using a nickel catalyst in chloroform at −10 °C, similar to our previously reported procedure (Figures 2A and S1B, C).[10] Based on the size-exclusion chromatography (SEC) analysis of the polymerization product (Figures 2B and S4), combined with the results of high-resolution atomic force microscopy (AFM) imaging (see Section 3.1 in the SI), the following findings can be drawn: (i) the polymerizations of **3** proceeded through the "transit-type MGR" mechanism and produced a 1-D supramolecular structure with the average length of 183 nm and a height of approximately 2 nm (Figures 2C–E, S2, and S3A; see also Section 3.2 in the SI);[20] (ii) in the resulting 1-D chain, the poly(**3**)-based macromolecular building blocks with a number-average molecular mass (M_n) of 1.9×10^4 g mol^{-1} (corresponding to a number-average degree of polymerization of approximately 26), which appeared as dot-like structures in the AFM image (Figure S5), were supramolecularly linked end-to-end through multiple intermolecular hydrogen bonding, as depicted in Figure 2A; and (iii) a single supramolecular chain was composed of approximately 70 macromolecular building blocks on average (Figure S3B), based on the fact that the length increment in the chain axis direction per single isocyanide unit in amino acid-based polyisocyanides was reported to be approximately 0.1 nm.[10,21]

We also confirmed that the dissociation of the supramolecular structure was accelerated by ultrasonic treatment (Figure S6), as observed in various supramolecular systems stabilized by hydrogen-bonding interactions.[22] For clarity, we have used the prefix "*supra*-" to describe as-synthesized polymerization products with a 1-D supramolecular structure in the following discussion. The thin-film X-ray diffraction (XRD) analysis suggested that the *supra*-poly(**3**) chains could be arranged in a hexagonal array with a lattice constant of a = 3.78 nm (Figure S7A; for a comparable result for completely dissociated poly(**3**), see Figure S7B). In contrast, the homopolymerization product synthesized from methyl-substituted optically active **2L** with the same BDT-based pendant (poly(**2L**) in Figure 3B) did not show a marked change in the SEC elution profile after treating with THF/DMSO (96:4, v/v) for 4 days (Figure S8). This result indicated that the chain-transfer reaction hardly occurred during the polymerization of **2L**, through which conventional covalent macromolecular chains could be produced.[23]

Chiroptical Properties of 1-D Supramolecular Polymers Containing Achiral and Chiral Units and Chiral Amplification. We next investigated chiral amplification in the preferred-handed helix formation, related to the "sergeants and soldiers" effect, based on circular dichroism (CD) spectral analyses of *supra*-poly(**3**$_{1-r}$-*co*-**2L**$_r$). Copolymerizations of **3** and **2L** at different feed ratios ([**3**]$_0$/[**2L**]$_0$ = 99:1, 90:10, 51:49, and 24:76) were conducted according to the procedure

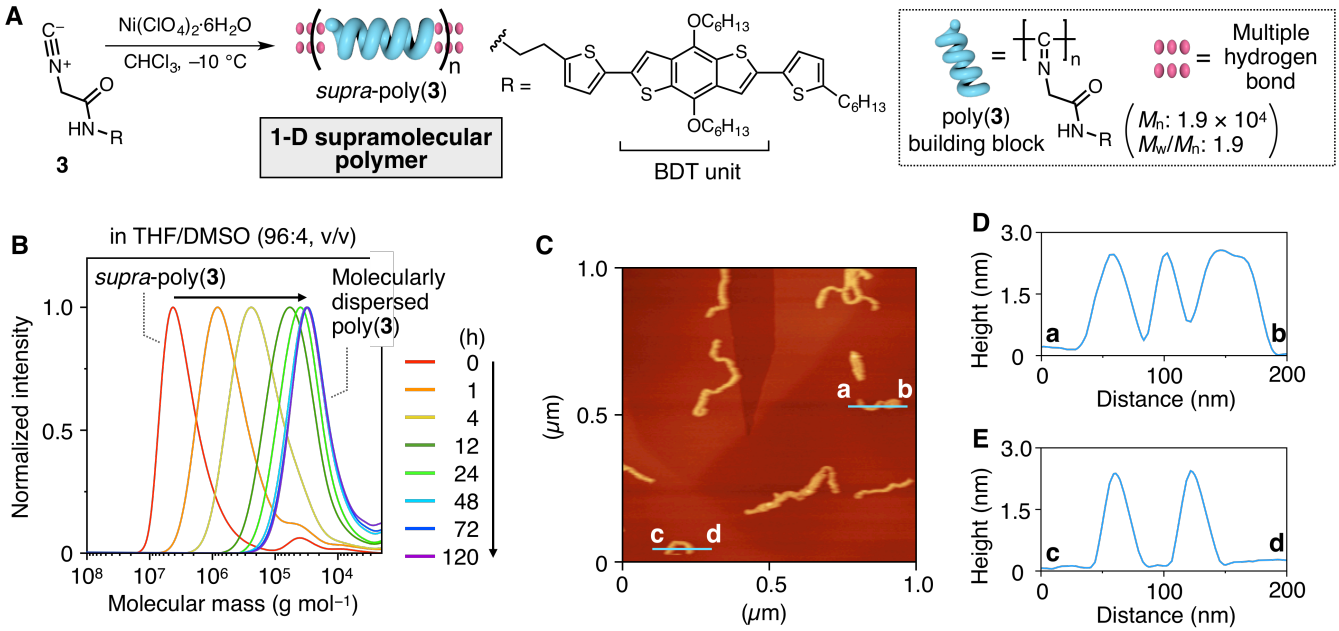

Figure 2. (A) Synthesis of 1-D supramolecular polymer (*supra*-poly(**3**)) through homopolymerization of a glycine-based isocyanide (**3**) with a nickel(II) catalyst in chloroform at −10 °C: $[\mathbf{3}]_0/[\mathrm{Ni}]_0 = 90$. (B) SEC monitoring of the disassociation process of *supra*-poly(**3**) while maintaining the completed reaction system at 25 °C after diluting 300-fold with THF/DMSO (96:4, v/v). Chromatograms show UV traces recorded at 254 nm. Column, TSKgel α-M with an estimated exclusion limit of 1×10^7 g mol^{-1}; eluent, THF containing 0.25 wt% tetrabutylammonium bromide; linear polystyrene standards. These conditions were used for the following SEC study. (C) Atomic force microscopy (AFM) image of *supra*-poly(**3**) on highly oriented pyrolytic graphite (HOPG) in air at ca. 20 °C. Observation area was 1.0×1.0 μm^2. (D,E) Height profiles measured along blue lines labeled a–b and c–d in (C) are shown in (D) and (E), respectively. Although the helical handedness of the polymer backbone was not controlled due to the absence of any chiral elements, the illustrations of helices shown here are represented as left-handed helices for the sake of simplicity.

described in Section 2.4 of the SI (Figure 3A). In all cases, both monomers were almost quantitatively consumed, as confirmed by HPLC analysis, and the as-synthesized products showed M_n values of more than 1.0×10^6 g mol^{-1} (Figure S10). Changes in the mole fraction of **2L** in the total residual monomers during copolymerization are also shown in Figure S11, which indicated that the copolymerizations of **3** and **2L** did not proceed in a random manner and that achiral **3** was preferentially inserted into the growing polymer chain over chiral **2L**.

For these copolymerization products, the SEC curves were apparently shifted rightward with varying degrees by dissociation treatment (Figure S10). For *supra*-poly($\mathbf{3}_{0.99}$-*co*-$\mathbf{2L}_{0.01}$), the SEC distribution after treating with THF for 120 h was shifted to almost the same region as that of completely dissociated poly(**3**) (Figure S10A). This indicated that the chain-transfer reaction occurred with approximately the same frequency as the homopolymerization of **3**. When the feed mole fractions of **3** were decreased by 90% and 51%, high-molecular mass components of more than 1×10^6 g mol^{-1} remained in the SEC charts after THF treatment (Figure S10B, C), which showed no further shift. A similar phenomenon was more markedly observed in the copolymerization system at $[\mathbf{3}]_0/[\mathbf{2L}]_0 = 24{:}76$ (Figure S10D). These results suggested that the chain-transfer constant in the copolymerization system decreased with an increasing mole fraction of alanine-based **2L**, which was reasonable owing to the polymerization behavior of **2L** without chain-transfer reactions, as mentioned above. The resulting 1-D supramolecular structure was partially dissociated and not perfectly maintained through typical purification/isolation processes, including precipitation, washing, and drying (Figure S12). Therefore, in this study, the completed polymerization systems were diluted with appropriate solvents, such as chloroform, THF, and a THF/DMSO mixture, and directly subjected to chromatographic and spectroscopic analysis, unless otherwise noted.

The resulting *supra*-poly($\mathbf{3}_{0.99}$-*co*-$\mathbf{2L}_{0.01}$), containing only one **2L** sergeant per hundred monomeric units, showed a clear CD in chloroform at −10 °C (Figure 3F), while the chiral **2L** monomer hardly showed the apparent Cotton effect (Figure S14A).[24] The pendant groups were most likely arranged in a one-handed helical array along the polyisocyanide-based 1-D supramolecular backbones (Figure 3D, E), thereby showing intense Cotton effects in the absorption regions of the BDT units. Furthermore, a clear CD signal was not observed for the molecularly dispersed poly($\mathbf{3}_{0.99}$-*co*-$\mathbf{2L}_{0.01}$) (Figure S14B), indicating that the conformational freedom of the macromolecular building blocks was likely restricted in the self-assembled state, and that a one-handed macromolecular helicity could be retained only in the 1-D supramolecular polymer. The copolymerization system containing 1 mol% of opposite enantiomeric sergeant **2D** in the feed afforded *supra*-poly($\mathbf{3}_{0.99}$-*co*-$\mathbf{2D}_{0.01}$) (Figure 3A), showing a split-type CD with the perfect mirror image of *supra*-poly($\mathbf{3}_{0.99}$-*co*-$\mathbf{2L}_{0.01}$) (Figure 3F). As the characteristic absorption bands of the polyisocyanide backbone (270–350 nm) and the BDT pendant (235–460 nm) were overlapped, the helix-sense excess of *supra*-poly($\mathbf{3}_{1-r}$-*co*-$\mathbf{2L}_r$) backbones could not be simply discussed from the CD data.[25] Onitsuka and Sato et al. reported a quantitative estimation of helix-sense selectivities for helical

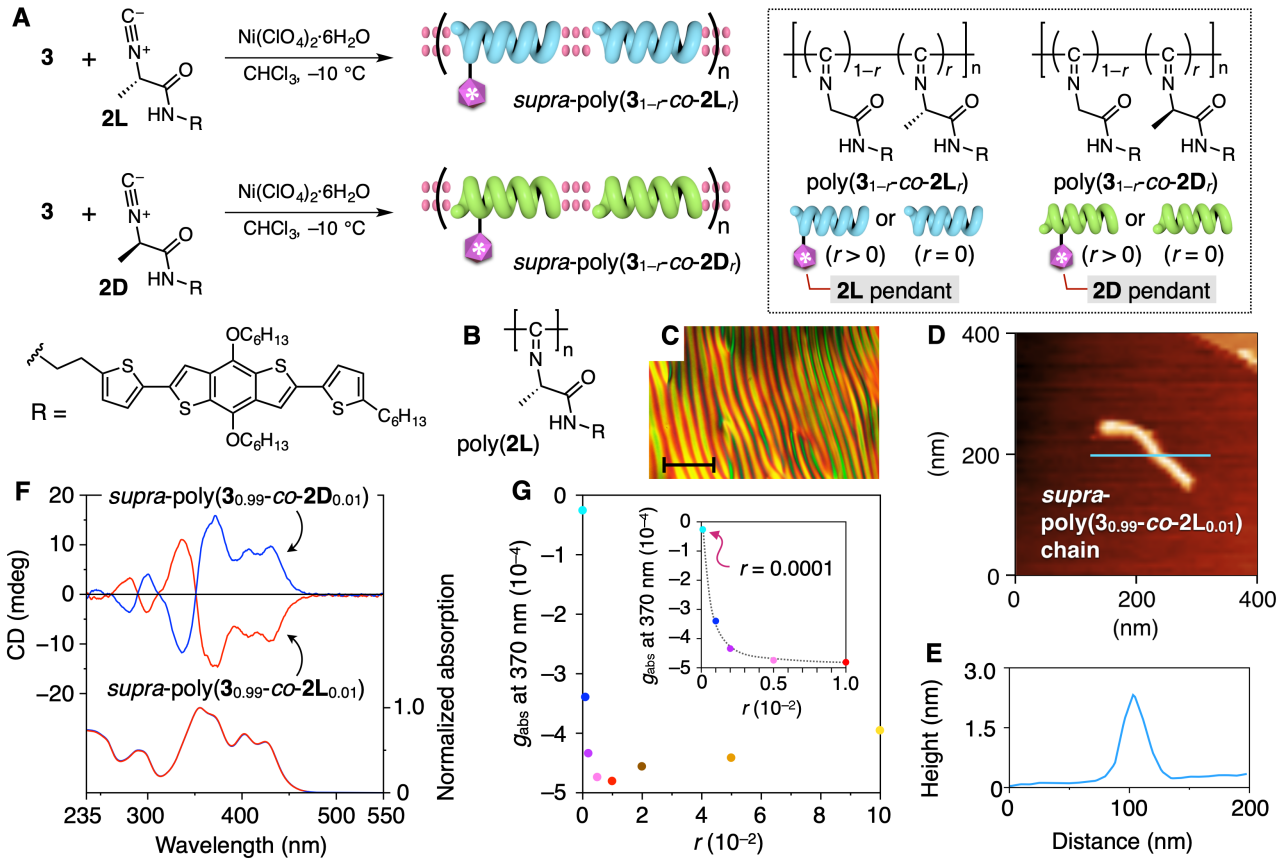

Figure 3. (A) Copolymerization of **3** with optically active monomer **2L** or **2D** using a nickel(II) catalyst in chloroform at –10 °C to afford *supra*-poly(**3**$_{1-r}$-*co*-**2L**$_r$) or *supra*-poly(**3**$_{1-r}$-*co*-**2D**$_r$), respectively. Molar feed ratios ([**3**]$_0$/[**2**]$_0$) were determined by HPLC using a CHIRALPAK IE-3 column (see Figure S9). (B) Structure of poly(**2L**) obtained through homopolymerization of **2L** under the same conditions as the reaction in (A). (C) Polarized optical micrograph of a cholesteric liquid crystalline phase of *supra*-poly(**3**$_{0.99}$-*co*-**2L**$_{0.01}$) in a concentrated chloroform solution (ca. 11 wt%) taken at room temperature (ca. 20 °C). Scale bar = 100 μm. (D) AFM image of *supra*-poly(**3**$_{0.99}$-*co*-**2L**$_{0.01}$) on HOPG in air at ca. 20 °C. Observation area was 400 × 400 nm^2 (see also Figure S15). (E) Height profile measured along a blue line in (D). (F) Absorption (lower) and CD (upper) spectra of *supra*-poly(**3**$_{0.99}$-*co*-**2L**$_{0.01}$) and *supra*-poly(**3**$_{0.99}$-*co*-**2D**$_{0.01}$). As controlling the solution concentration was difficult, resulting from the slight instability of supramolecular structures during isolation, CD spectra were normalized to the absorbance at the absorption maximum wavelength (for data validation, see Figure S13 and Section 3.3 in the SI). (G) Plots of g_{abs} values at the CD maximum wavelength (370 nm) as a function of the proportion of **2L** units in *supra*-poly(**3**$_{1-r}$-*co*-**2L**$_r$) (for corresponding spectral data, see Figure S19). The results in the range of r = 0.0001–0.01 are also shown in the inset for clarity. Each plot is color-coded, as defined in Figure S19.

polyisocyanides,[26] in which helical handedness was determined during polymerization and not inverted after polymerization, as was the case in the present study. From this report, a helix-sense excess of non-dynamical helical polyisocyanides can be defined on the basis of the excess free energy of activation for a helix reversal reaction, which becomes larger at lower polymerization temperatures. Therefore, the helix-sense excess that is correlated with the CD intensity increases with decreasing temperature until a macromolecular helicity is completely controlled. Accordingly, if the CD spectrum is unchanged despite a further decrease in polymerization temperature, the polymer backbone possesses a perfect one-handed helical conformation. To investigate the helix-sense excess of *supra*-poly(**3**$_{0.99}$-*co*-**2L**$_{0.01}$), the chiroptical properties of the supramolecular polymers obtained through copolymerizations of **3** and **2L** ([**3**]$_0$/[**2L**]$_0$ = 99:1) at different temperatures (–30, –10, and 20 °C) were compared (Figure S16). The CD value of *supra*-poly(**3**$_{0.99}$-*co*-**2L**$_{0.01}$) synthesized at 20 °C was slightly lower than that obtained at –10 °C, while no significant difference was observed between the results obtained at –30 and –10 °C. These results led to the conclusion that almost all macromolecular building blocks in *supra*-poly(**3**$_{0.99}$-*co*-**2L**$_{0.01}$) prepared below –10 °C adopted a one-handed helical conformation. Furthermore, the 1-D supramolecular structure and helical chirality of *supra*-poly(**3**$_{0.99}$-*co*-**2L**$_{0.01}$) were stably maintained as long as the sample was stored in chloroform at –10 °C, which was confirmed by the SEC curve and the chiroptical property of *supra*-poly(**3**$_{0.99}$-*co*-**2L**$_{0.01}$) remaining unchanged after allowing to stand for 72 h (Figure S17).

The CD spectral pattern of *supra*-poly(**3**$_{0.99}$-*co*-**2L**$_{0.01}$) was almost a mirror image of poly(**2L**) and *supra*-poly(**3**$_{0.24}$-*co*-**2L**$_{0.76}$), containing a large amount of chiral unit (r = 0.76), although their absolute intensities were different (Figure S18). This chiroptical inversion depending on the achiral/chiral isocyanide compositions was also observed in our previous study using **1A**$_a$ and **1L**$_a$.[10] Both the macromolecular helicity of

the polyisocyanide chains and the chiral arrangement manner of the BDT pendants in *supra*-poly(**3**$_{0.99}$-*co*-**2L**$_{0.01}$) were likely the opposite of those in poly(**2L**). The inconsistency in the absolute CD intensities was probably due to differences in their chiral arrangements of BDT pendants along the helical backbones, as reported previously.[19,27] We also confirmed that *supra*-poly(**3**$_{0.99}$-*co*-**2L**$_{0.01}$) showed the highest Kuhn's dissymmetry factor (g_{abs}) among *supra*-poly(**3**$_{1-r}$-*co*-**2L**$_r$) with r = 0.0001–0.10 (Figure 3G). Thus, *supra*-poly(**3**$_{0.99}$-*co*-**2L**$_{0.01}$) with an almost perfect one-handed helicity was mainly used in subsequent CPL experiments.

Generation of Circularly Polarized Light through Hierarchical Chiral Amplification. We next investigated the CPL features of *supra*-poly(**3**$_{1-r}$-*co*-**2L**$_r$) in solution and film states. The photoluminescence (PL), CPL, and luminescence dissymmetry factor (g_{lum}) spectra of *supra*-poly(**3**$_{1-r}$-*co*-**2L**$_r$) are shown in Figure 4A. Here, g_{lum} is defined as $2(I_L - I_R)/(I_L + I_R)$, where I_L and I_R are the PL intensities of the left- and right-handed circularly polarized light, respectively. The *supra*-poly(**3**$_{0.99}$-*co*-**2L**$_{0.01}$) film prepared by drop-coating the chloroform solution onto a quartz plate, in which the supramolecular chains were hexagonally packed (Figure S20A), exhibited a clear CPL signal in the fluorescence region of the BDT pendant unit (for repeatability and stability, see Figures S21 and S22, respectively),[28] while the chloroform solution of *supra*-poly(**3**$_{0.99}$-*co*-**2L**$_{0.01}$) did not. We also confirmed that the mirror-imaged CPL spectrum was observed for the *supra*-poly(**3**$_{0.99}$-*co*-**2D**$_{0.01}$) film (blue lines in Figure 4A) and that the drop-cast films prepared from *supra*-poly(**3**), consisting entirely of achiral units, and from completely dissociated poly(**3**$_{0.99}$-*co*-**2L**$_{0.01}$) did not produce an apparent CPL (Figure S24). Therefore, we can reliably state that the CPL materials could be produced from a tiny amount of chiral source by taking advantage of chiral amplification in the present 1-D supramolecular system. The emission maximum wavelength in the film state was red-shifted and broadened compared with the result in chloroform, which was due to the elongated π-conjugation length. We found that *supra*-poly(**3**$_{0.99}$-*co*-**2L**$_{0.01}$) formed a lyotropic cholesteric liquid crystalline phase in the concentrated chloroform solution (ca. 11 wt%) (Figure 3C), suggesting that further supramolecular helical assembly of the 1-D supramolecular fibers was likely key to producing the CPL. Notably, *supra*-poly(**3**$_{0.9999}$-*co*-**2L**$_{0.0001}$), containing only 0.01 mol% of chiral **2L** unit, also showed an observable CPL signal owing to exquisite chiral amplification (Figure 4A). Interestingly, poly(**2L**) hardly showed a CPL signal (Figure S25). This result was in stark contrast to those of conventional chiral materials developed through the sergeants-and-soldiers-type chiral amplification, in which the performances of materials containing achiral/chiral components were less than or comparable to those consisting entirely of a chiral component.[7-9] The reason for this is unclear at present, but the difference in the chiral arrangement of the BDT unit, as discussed above, and/or the lack of lyotropic liquid crystallinity in poly(**2L**) (Figure S26), which caused the disordered arrangement in the film state as evidenced by the XRD analysis (Figure S20C), might be related to too many sergeants spoiling the CPL.

Much to our disappointment, the emission from the *supra*-poly(**3**$_{1-r}$-*co*-**2L**$_r$)-based films was quite weak and could not be recognized by the naked eye under irradiation at 365 nm, although the corresponding monomers (**3** and **2L**) showed the apparent solid-state PL, as shown in Figure S27. This was

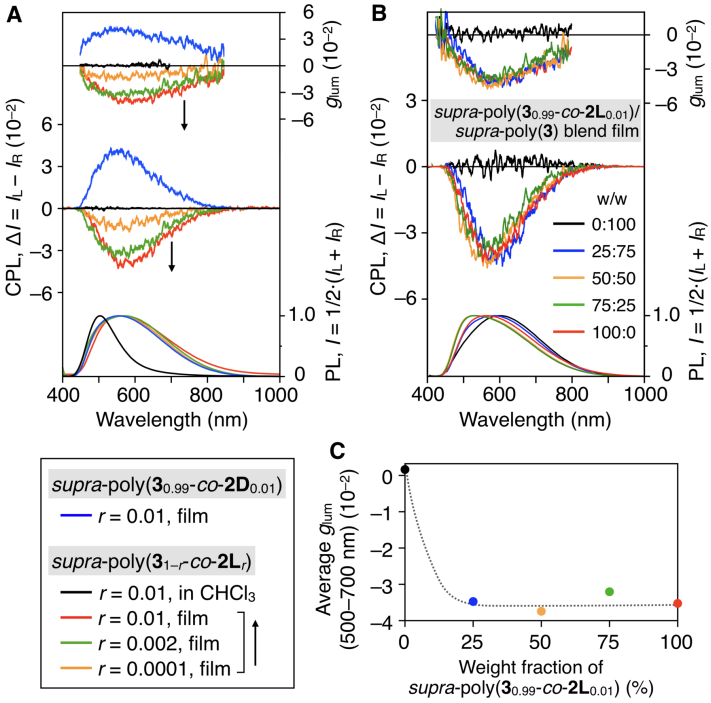

Figure 4. (A,B) PL (bottom), CPL (middle), and g_{lum} (top) spectra of (A) *supra*-poly(**3**$_{1-r}$-*co*-**2L**$_r$) (r = 0.01, 0.002, and 0.0001) and *supra*-poly(**3**$_{0.99}$-*co*-**2D**$_{0.01}$) in chloroform and/or film states and (B) *supra*-poly(**3**$_{0.99}$-*co*-**2L**$_{0.01}$)/*supra*-poly(**3**) blend films with different compositions at room temperature (ca. 20 °C); λ_{ex} = 350 nm. (C) Plots of average g_{lum} values in the range of 500–700 nm as a function of the weight fraction of *supra*-poly(**3**$_{0.99}$-*co*-**2L**$_{0.01}$) in blend films. Each plot is color-coded as defined in (B).

probably due to the BDT pendants existing on every carbon atom in the main-chain and being arranged too densely alongside each other, which might cause intramolecular fluorescence quenching.[29] Meanwhile, it was a pleasant surprise to discover a unique CPL generation through additional chiral amplification, achieved by mixing the chiral and achiral 1-D supramolecular fibers (Figure 4B, C). The blend films consisting of *supra*-poly(**3**$_{0.99}$-*co*-**2L**$_{0.01}$) and *supra*-poly(**3**) (25:75, w/w) showed a comparable CPL intensity to that of pure *supra*-poly(**3**$_{0.99}$-*co*-**2L**$_{0.01}$). This result was beyond our expectations because chiral amplification in the preferred-handed helix formation did not occur between supramolecular fibers in solution (Figure S28 and Section 3.4 in the SI). Based on this finding, we envisaged that circularly polarized light of the desired color could be produced through chiral transfer from *supra*-poly(**3**$_{0.99}$-*co*-**2L**$_{0.01}$) to achiral fluorescent dyes in the film state. To this end, we prepared a series of blend films showing red, green, and blue emissions through slow evaporation of a solution of *supra*-poly(**3**$_{0.99}$-*co*-**2L**$_{0.01}$) (23 mg mL^{-1}) in chloroform in the presence of different achiral fluorescent dyes (Cy3, TPE, and ANT, respectively; Figure 5A). We confirmed that the co-assembled dye did not significantly affect the hexagonal packing of the *supra*-poly(**3**$_{0.99}$-*co*-**2L**$_{0.01}$) chains in the film (Figure S20B). Each blend film showed a clear fluorescence that was visible to the naked eye and exhibited intense CPL signals in the corresponding PL regions of the achiral dyes (Figure 5B). The maximum $|g_{lum}|$ values were slightly lower than that of the *supra*-poly(**3**$_{0.99}$-*co*-**2L**$_{0.01}$) film, but reached more than 2.0 × 10^{-2}. These results indicated that

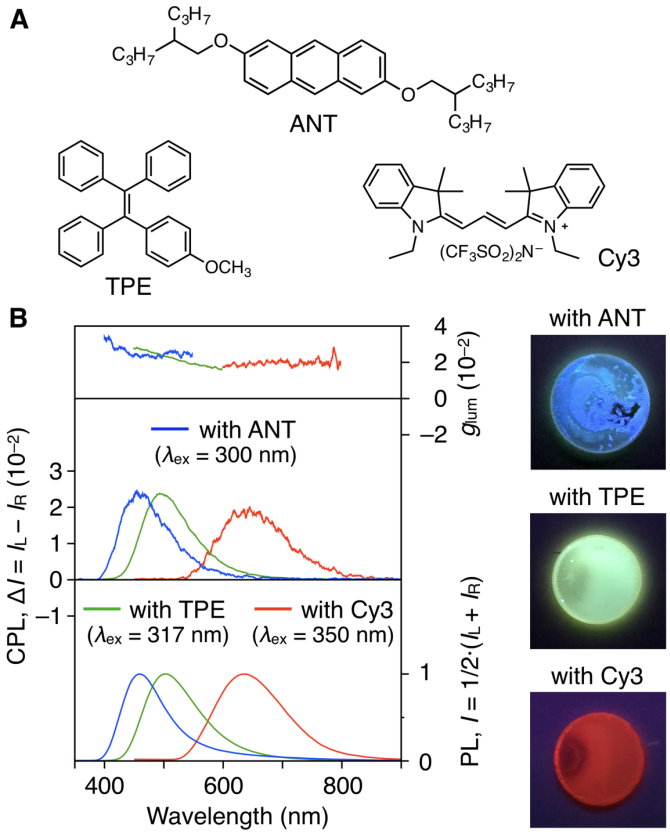

Figure 5. (A) Structures of achiral fluorescent dyes (ANT, TPE, and Cy3). (B) PL (bottom), CPL (middle), and g_{lum} (top) spectra of *supra*-poly(**3**$_{0.99}$-*co*-**2L**$_{0.01}$)-based blend films containing ANT (polymer/dye = 7:3, w/w), TPE (polymer/dye = 6:4, w/w), and Cy3 (polymer/dye = 6:4, w/w) at room temperature (ca. 20 °C). Photographs of the corresponding blend films under irradiation at 365 nm are also shown on the right side. The influence of optical anisotropy on the blend films was confirmed to be almost negligible (see Figure S29).

the chiral information in *supra*-poly(**3**$_{0.99}$-*co*-**2L**$_{0.01}$) was efficiently transferred and amplified to the achiral fluorescent dyes in blend films (for the induced CPL study using *supra*-poly(**3**$_{0.99}$-*co*-**2D**$_{0.01}$)-based blend films, see Figure S30). Again, the blend films prepared from *supra*-poly(**3**) and poly(**2L**) did not produce any circularly polarized light derived from the achiral dye (Figure S31). When the fluorescent blend film was prepared from the previously reported *supra*-poly(**1A**$_{a0.99}$-*co*-**1L**$_{a0.01}$) containing an oligothiophene pendant (see Figure 1A) and the achiral dye, the clear CPL was not observed (Figure S32). Therefore, the unusual CPL from hierarchical chiral amplification would be an anomalous phenomenon that occurred only in the blend films containing *supra*-poly(**3**$_{1-r}$-*co*-**2L**$_r$) with a BDT pendant unit. The fused aromatic ring system of BDT might take part in favorable π–π interactions with fluorescent π-conjugated guest molecules.

CONCLUSIONS

We have synthesized 1-D self-assembled supramolecular fibers, in which the BDT-appended helical macromolecular building blocks were noncovalently connected end-to-end, through polymerization via the "transit-type MGR" mechanism. The helical handedness of all macromolecular building blocks in the supramolecular system was almost perfectly controlled by a tiny amount of the chiral unit (1 mol%) through strong chiral amplification. The one-handed helical supramolecular fibers were further helically assembled in the film state and showed a CPL signal in the fluorescence region of the BDT unit. Although the emission intensity was low, notably, the supramolecular system containing 0.01 mol% of chiral unit (*supra*-poly(**3**$_{0.9999}$-*co*-**2L**$_{0.0001}$)) also generated circularly polarized light at a detectable level, while no CPL was observed for the corresponding chiral homopolymer film. Gratifyingly, when the chiral supramolecular fibers were mixed with achiral fluorophores, additional chiral amplification occurred in the blend films through chiral transfer from the helically assembled supramolecular system to achiral guests. As a result, the achiral fluorophores were chirally arranged in the blend film and showed the induced CPL with $|g_{lum}|$ values greater than 1.0×10^{-2}. Importantly, the color of CPL could be tuned from blue to red by simply changing the achiral dyes blended with our chiral supramolecular system. The present results demonstrate that a series of chiral functional materials, including chiral sensors, chiral stationary phases, and asymmetric catalysts, could also be produced from an infinitesimal chiral source by taking advantage of this hierarchical chiral amplification system.

ASSOCIATED CONTENT

Supporting Information

The Supporting Information is available free of charge on the ACS Publications website.

Experimental procedures, characterizations of monomers and polymers, and additional spectroscopic, chromatographic, and microscopic data (PDF)

AUTHOR INFORMATION

Corresponding Author

*E-mail: ikai@chembio.nagoya-u.ac.jp

Notes

The authors declare no competing financial interest.

ACKNOWLEDGMENT

This work was supported by the Japan Society for the Promotion of Science (JSPS) KAKENHI Grant No. 17K05875 (Grant-in-Aid for Scientific Research (C)), 17J01940 (Research Fellowship for Young Scientists), and 18H05209 (Grant-in-Aid for Specially Promoted Research). We are appreciative of Prof. Tetsuya Taima (Kanazawa University) for the XRD analysis and Dr. Tatsuya Nishimura (Kanazawa University) for preparing a cholesteric liquid crystal film.

REFERENCES

(1) (a) Bonner, W. A. The Origin and Amplification of Biomolecular Chirality. *Origins Life Evol. Biospheres* **1991**, *21*, 59–111. (b) Feringa, B. L.; van Delden, R. A. Absolute Asymmetric Synthesis: The Origin, Control, and Amplification of Chirality. *Angew. Chem., Int. Ed.* **1999**, *38*, 3418–3438. (c) Weissbuch, I.; Leiserowitz, L.; Lahav, M. Stochastic "Mirror Symmetry Breaking" via Self-Assembly, Reactivity and Amplification of Chirality: Relevance to Abiotic Conditions. *Top. Curr. Chem.* **2005**, *259*, 123–165. (d) Blanco, C.; Hochberg, D. Stochastic Mirror Symmetry Breaking: Theoretical Models and Simulation of Experiments. *Top. Curr. Chem.* **2012**, *333*, 157–211.

(2) (a) Girard, C.; Kagan, H. B. Nonlinear Effects in Asymmetric Synthesis and Stereoselective Reactions: Ten Years of Investigation. *Angew. Chem., Int. Ed.* **1998**, *37*, 2923–2959. (b) Satyanarayana, T.;

Abraham, S.; Kagan, H. B. Nonlinear Effects In Asymmetric Catalysis. *Angew. Chem., Int. Ed.* **2009**, *48*, 456–494. (c) Bissette, A. J.; Fletcher, S. P. Mechanisms of Autocatalysis. *Angew. Chem., Int. Ed.* **2013**, *52*, 12800–12826. (d) Soai, K.; Kawasaki, T.; Matsumoto, A. Asymmetric Autocatalysis of Pyrimidyl Alkanol and Its Application to the Study on the Origin of Homochirality. *Acc. Chem. Res.* **2014**, *47*, 3643–3654. (e) Gellman, A. J.; Ernst, K.-H. Chiral Autocatalysis and Mirror Symmetry Breaking. *Catal. Lett.* **2018**, *148*, 1610–1621.

(3) Green, M. M.; Reidy, M. P.; Johnson, R. J.; Darling, G.; O'leary, D. J.; Willson, G. Macromolecular Stereochemistry: The Out-of-Proportion Influence of Optically Active Comonomers on the Conformational Characteristics of Polyisocyanates. The Sergeants and Soldiers Experiment. *J. Am. Chem. Soc.* **1989**, *111*, 6452–6454.

(4) (a) Green, M. M.; Park, J.-W.; Sato, T.; Teramoto, A.; Lifson, S.; Selinger, R. L. B.; Selinger, J. V. The Macromolecular Route to Chiral Amplification. *Angew. Chem., Int. Ed.* **1999**, *38*, 3138–3154. (b) Jain, V.; Cheon, K.-S.; Tang, K.; Jha, S.; Green, M. M. Chiral Cooperativity in Helical Polymers. *Isr. J. Chem.* **2011**, *51*, 1067–1074.

(5) (a) Green, M. M.; Peterson, N. C.; Sato, T.; Teramoto, A.; Cook, R.; Lifson, S. A Helical Polymer with a Cooperative Response to Chiral Information. *Science* **1995**, *268*, 1860–1866. (b) Sato, T.; Terao, K.; Teramoto, A.; Fujiki, M. Molecular Properties of Helical Polysilylenes in Solution. *Polymer* **2003**, *44*, 5477–5495. (c) Yashima, E.; Maeda, K.; Nishimura, T. Detection and Amplification of Chirality by Helical Polymers. *Chem. - Eur. J.* **2004**, *10*, 42–51. (d) Maeda, K.; Yashima, E. Dynamic Helical Structures: Detection and Amplification of Chirality. *Top. Curr. Chem.* **2006**, *265*, 47–88. (e) Fujiki, M. Mirror Symmetry Breaking of Silicon Polymers-From Weak Bosons to Artificial Helix. *Chem. Rec.* **2009**, *9*, 271–298. (f) Yashima, E.; Maeda, K.; Iida, H.; Furusho, Y.; Nagai, K. Helical Polymers: Synthesis, Structures, and Functions. *Chem. Rev.* **2009**, *109*, 6102–6211. (g) Yashima, E.; Ousaka, N.; Taura, D.; Shimomura, K.; Ikai, T.; Maeda, K. Supramolecular Helical Systems: Helical Assemblies of Small Molecules, Foldamers, and Polymers with Chiral Amplification and Their Functions. *Chem. Rev.* **2016**, *116*, 13752–13990. (h) Freire, F.; Quiñoá, E.; Riguera, R. Supramolecular Assemblies from Poly(phenylacetylene)s. *Chem. Rev.* **2016**, *116*, 1242–1271.

(6) (a) Mateos-Timoneda, M. A.; Crego-Calama, M.; Reinhoudt, D. N. Supramolecular Chirality of Self-Assembled Systems in Solution. *Chem. Soc. Rev.* **2004**, *33*, 363–372. (b) Palmans, A. R. A.; Meijer, E. W. Amplification of Chirality in Dynamic Supramolecular Aggregates. *Angew. Chem., Int. Ed.* **2007**, *46*, 8948–8968. (c) Pijper, D.; Feringa, B. L. Control of Dynamic Helicity at the Macro- and Supramolecular Level. *Soft Matter* **2008**, *4*, 1349–1372. (d) Ho, R. M.; Chiang, Y. W.; Lin, S. C.; Chen, C. K. Helical Architectures from Self-Assembly of Chiral Polymers and Block Copolymers. *Prog. Polym. Sci.* **2011**, *36*, 376–453. (e) Zhang, D.-W.; Zhao, X.; Li, Z.-T. Aromatic Amide and Hydrazide Foldamer-Based Responsive Host-Guest Systems. *Acc. Chem. Res.* **2014**, *47*, 1961–1970. (f) Dorca, Y.; Greciano, E. E.; Valera, J. S.; Gómez, R.; Sánchez, L. Hierarchy of Asymmetry in Chiral Supramolecular Polymers: Toward Functional, Helical Supramolecular Structures. *Chem. - Eur. J.* **2019**, *25*, 5848–5864.

(7) (a) Reggelin, M.; Doerr, S.; Klussmann, M.; Schultz, M.; Holbach, M. Helically Chiral Polymers: A Class of Ligands for Asymmetric Catalysis. *Proc. Natl. Acad. Sci. U. S. A.* **2004**, *101*, 5461–5466. (b) Raynal, M.; Portier, F.; van Leeuwen, P. W. N. M.; Bouteiller, L. Tunable Asymmetric Catalysis through Ligand Stacking in Chiral Rigid Rods. *J. Am. Chem. Soc.* **2013**, *135*, 17687–17690. (c) Ke, Y.-Z.; Nagata, Y.; Yamada, T.; Suginome, M. Majority-Rules-Type Helical Poly(quinoxaline-2,3-diyl)s as Highly Efficient Chirality-Amplification Systems for Asymmetric Catalysis. *Angew. Chem., Int. Ed.* **2015**, *54*, 9333–9337. (d) Nagata, Y.; Nishikawa, T.; Suginome, M. Exerting Control over the Helical Chirality in the Main Chain of Sergeants-and-Soldiers-Type Poly(quinoxaline-2,3-diyl)s by Changing from Random to Block Copolymerization Protocols. *J. Am. Chem. Soc.* **2015**, *137*, 4070–4073. (e) Takata, L. M. S.; Iida, H.; Shimomura, K.; Hayashi, K.; dos Santos, A. A.; Yashima, E. Helical Poly(phenylacetylene) Bearing Chiral and Achiral Imidazolidinone-Based Pendants that Catalyze Asymmetric Reactions due to Catalytically Active Achiral Pendants Assisted by Macromolecular Helicity. *Macromol. Rapid Commun.* **2015**, *36*, 2047–2054. (f) Desmarchelier, A.; Caumes, X.; Raynal, M.; Vidal-Ferran, A.; van Leeuwen, P. W. N. M.; Bouteiller, L. Correlation between the Selectivity and the Structure of an Asymmetric Catalyst Built on a Chirally Amplified Supramolecular Helical Scaffold. *J. Am. Chem. Soc.* **2016**, *138*, 4908–4916. (g) Nagata, Y.; Nishikawa, T.; Suginome, M. Solvent Effect on the Sergeants-and-Soldiers Effect Leading to Bidirectional Induction of Single-Handed Helical Sense of Poly(quinoxaline-2,3-diyl)s Copolymers in Aromatic Solvents. *ACS Macro Lett.* **2016**, *5*, 519–522. (h) Li, Y.; Bouteiller, L.; Raynal, M. Catalysts Supported by Homochiral Molecular Helices: A New Concept to Implement Asymmetric Amplification in Catalytic Science. *ChemCatChem* **2019**, *11*, 5212–5226.

(8) (a) Jung, J. H.; Moon, S.-J.; Ahn, J.; Jaworski, J.; Shinkai, S. Controlled Supramolecular Assembly of Helical Silica Nanotube–Graphene Hybrids for Chiral Transcription and Separation. *ACS Nano* **2013**, *7*, 2595–2601. (b) Fang, Y.; Ghijsens, E.; Ivasenko, O.; Cao, H.; Noguchi, A.; Mali, K. S.; Tahara, K.; Tobe, Y.; De Feyter, S. Dynamic Control over Supramolecular Handedness by Selecting Chiral Induction Pathways at the Solution–Solid Interface. *Nat. Chem.* **2016**, *8*, 711–717.

(9) (a) Ikai, T.; Shimizu, S.; Awata, S.; Shinohara, K. Chiral Amplification in π-Conjugated Helical Polymers with Circularly Polarized Luminescence. *Macromolecules* **2018**, *51*, 2328−2334. (b) Nagata, Y.; Nishikawa, T.; Suginome, M. Abnormal Sergeants-and-Soldiers Effects of Poly(quinoxaline-2,3-diyl)s Enabling Discrimination of One-Carbon Homologous *n*-Alkanes through a Highly Sensitive Solvent-Dependent Helix Inversion. *Chem.Commun.* **2018**, *54*, 6867–6870.

(10) Wada, Y.; Shinohara, K.; Asakawa, H.; Matsui, S.; Taima, T.; Ikai, T. One-Step Synthesis of One-Dimensional Supramolecular Assemblies Composed of Helical Macromolecular Building Blocks. *J. Am. Chem. Soc.* **2019**, *141*, 13995−14002.

(11) (a) Richardson, F. S.; Riehl, J. P. Circularly Polarized Luminescence Spectroscopy. *Chem. Rev.* **1977**, *77*, 773–792. (b) Riehl, J. P.; Richardson, F. S. Circularly Polarized Luminescence Spectroscopy. *Chem. Rev.* **1986**, *86*, 1–16. (c) Longhi, G.; Castiglioni, E.; Koshoubu, J.; Mazzeo, G.; Abbate, S. Circularly Polarized Luminescence: A Review of Experimental and Theoretical Aspects. *Chirality* **2016**, *28*, 696–707.

(12) (a) Parker, D.; Dickins, R. S.; Puschmann, H.; Crossland, C.; Howard, J. A. K. Being Excited by Lanthanide Coordination Complexes: Aqua Species, Chirality, Excited-State Chemistry, and Exchange Dynamics. *Chem. Rev.* **2002**, *102*, 1977–2010. (b) Tsukube, H.; Shinoda, S. Lanthanide Complexes in Molecular Recognition and Chirality Sensing of Biological Substrates. *Chem. Rev.* **2002**, *102*, 2389–2404. (c) Bünzli, J.-C. G.; Piguet, C. Taking Advantage of Luminescent Lanthanide Ions. *Chem. Soc. Rev.* **2005**, *34*, 1048–1077. (d) Muller, G. Luminescent Chiral Lanthanide(III) Complexes as Potential Molecular Probes. *Dalton Trans.* **2009**, 9692–9707. (e) Carr, R.; Evans, N. H.; Parker, D. Lanthanide Complexes as Chiral Probes Exploiting Circularly Polarized Luminescence. *Chem. Soc. Rev.* **2012**, *41*, 7673–7686. (f) Heffern, M. C.; Matosziuk, L. M.; Meade, T. J. Lanthanide Probes for Bioresponsive Imaging. *Chem. Rev.* **2014**, *114*, 4496–4539. (g) Zinna, F.; Di Bari, L. Lanthanide Circularly Polarized Luminescence: Bases and Applications. *Chirality* **2015**, *27*, 1–13. (h) Barry, D. E.; Caffrey, D. F.; Gunnlaugsson, T. Lanthanide-Directed Synthesis of Luminescent Self-Assembly Supramolecular Structures and Mechanically Bonded Systems from Acyclic Coordinating Organic Ligands. *Chem. Soc. Rev.* **2016**, *45*, 3244–3274.

(13) (a) Emeis, C. A.; Oosterhoff, L. J. Emission of Circularly-Polarised Radiation by Optically-Active Compounds. *Chem. Phys. Lett.* **1967**, *1*, 129–132. (b) Sánchez-Carnerero, E. M.; Agarrabeitia, A. R.; Moreno, F.; Maroto, B. L.; Muller, G.; Ortiz, M. J.; de la Moya, S. Circularly Polarized Luminescence from Simple Organic Molecules. *Chem. - Eur. J.* **2015**, *21*, 13488–13500. (c) Chen, N.; Yan, B. Recent Theoretical and Experimental Progress in Circularly Polarized Luminescence of Small Organic Molecules. *Molecules* **2018**, *23*. (d) Han, J.; Guo, S.; Lu, H.; Liu, S.; Zhao, Q.; Huang, W. Recent Progress on Circularly Polarized Luminescent Materials for Organic Optoelectronic Devices. *Adv. Opt. Mater.* **2018**, *6*, 1800538. (e) Tanaka, H.; Inoue, Y.; Mori, T. Circularly Polarized Luminescence and Circular Dichroisms in Small Organic Molecules: Correlation between Excitation and Emission Dissymmetry Factors. *ChemPhotoChem* **2018**, *2*, 386–402. (f) Ma, J.-L.; Peng, Q.; Zhao, C.-H. Circularly Polarized Luminescence Switching in Small Organic Molecules. *Chem. - Eur. J.* **2019**, *25*, 15441–15454.

(14) (a) Kumar, J.; Nakashima, T.; Kawai, T. Circularly Polarized Luminescence in Chiral Molecules and Supramolecular Assemblies. *J. Phys. Chem. Lett.* **2015**, *6*, 3445–3452. (b) Liu, M.; Zhang, L.; Wang, T. Supramolecular Chirality in Self-Assembled Systems. *Chem. Rev.* **2015**, *115*, 7304–7397. (c) Mei, J.; Leung, N. L. C.; Kwok, R. T. K.; Lam, J. W. Y.; Tang, B. Z. Aggregation-Induced Emission: Together We Shine, United We Soar! *Chem. Rev.* **2015**, *115*, 11718–11940. (d) Roose, J.; Tang, B. Z.; Wong, K. S. Circularly-Polarized Luminescence (CPL) from Chiral AIE Molecules and Macrostructures. *Small* **2016**, *12*, 6495–6512. (e) Zhang, L.; Wang, T.; Shen, Z.; Liu, M. Chiral Nanoarchitectonics: Towards the Design, Self-Assembly, and Function of Nanoscale Chiral Twists and Helices. *Adv. Mater.* **2016**, *28*, 1044–1059. (f) Xing, P.; Zhao, Y. Controlling

Supramolecular Chirality in Multicomponent Self-Assembled Systems. *Acc. Chem. Res.* **2018**, *51*, 2324–2334. (g) Li, H.; Li, B. S.; Tang, B. Z. Molecular Design, Circularly Polarized Luminescence, and Helical Self-Assembly of Chiral Aggregation-Induced Emission Molecules. *Chem. - Asian J.* **2019**, *14*, 674–688. (h) Sang, Y.; Han, J.; Zhao, T.; Duan, P.; Liu, M. Circularly Polarized Luminescence in Nanoassemblies: Generation, Amplification, and Application. *Adv. Mater.* **2019**, 1900110.

(15) (a) Watanabe, K.; Akagi, K. Helically Assembled π-Conjugated Polymers with Circularly Polarized Luminescence. *Sci. Technol. Adv. Mater.* **2014**, *15*, 044203. (b) Hu, R.; Kang, Y.; Tang, B. Z. Recent Advances in AIE Polymers. *Polym. J.* **2016**, *48*, 359–370. (c) Ikai, T. The Dawn of Chiral Material Development Using Saccharide-Based Helical Polymers. *Polym. J.* **2017**, *49*, 355–362. (d) Akagi, K. Interdisciplinary Chemistry Based on Integration of Liquid Crystals and Conjugated Polymers: Development and Progress. *Bull. Chem. Soc. Jpn.* **2019**, *92*, 1509–1655.

(16) Shen, Z.; Wang, T.; Shi, L.; Tang, Z.; Liu, M. Strong Circularly Polarized Luminescence from the Supramolecular Gels of an Achiral Gelator: Tunable Intensity and Handedness. *Chem. Sci.* **2015**, *6*, 4267–4272.

(17) Chen, S. H.; Katsis, D.; Schmid, A. W.; Mastrangelo, J. C.; Tsutsui, T.; Blanton, T. N. Circularly Polarized Light Generated by Photoexcitation of Luminophores in Glassy Liquid-Crystal Films. *Nature* **1999**, *397*, 506–508.

(18) Wada, Y.; Shinohara, K.; Ikai, T. Optically Active Triptycenes Containing Hexa-*peri*-hexabenzocoronene Units. *Chem. Commun.* **2019**, *55*, 11386–11389.

(19) Ikai, T.; Suzuki, D.; Shinohara, K.; Maeda, K.; Kanoh, S. A Cellulose-Based Chiral Fluorescent Sensor for Aromatic Nitro Compounds with Central, Axial and Planar Chirality. *Polym. Chem.* **2017**, *8*, 2257–2265.

(20) If a fiber had a too-elongated geometry and part of the chain structure was entangled, its length information could not be obtained and counted to estimate the average length. Therefore, the average length evaluated here is considered an underestimated value, and longer structures than the estimate would be produced in practice.

(21) (a) Cornelissen, J. J. L. M.; Donners, J. J. J. M.; de Gelder, R.; Graswinckel, W. S.; Metselaar, G. A.; Rowan, A. E.; Sommerdijk, N. A. J. M.; Nolte, R. J. M. β-Helical Polymers from Isocyanopeptides. *Science* **2001**, *293*, 676–680. (b) De Witte, P. A. J.; Hernando, J.; Neuteboom, E. E.; Van Dijk, E. M. H. P.; Meskers, S. C. J.; Janssen, R. A. J.; Van Hulst, N. F.; Nolte, R. J. M.; García-Parajó, M. F.; Rowan, A. E. Synthesis and Characterization of Long Perylenediimide Polymer Fibers: From Bulk to the Single-Molecule Level. *J. Phys. Chem. B* **2006**, *110*, 7803–7812.

(22) (a) Brunsveld, L.; Vekemans, J.; Hirschberg, J.; Sijbesma, R. P.; Meijer, E. W. Hierarchical Formation of Helical Supramolecular Polymers via Stacking of Hydrogen-Bonded Pairs in Water. *Proc. Natl. Acad. Sci. U. S. A.* **2002**, *99*, 4977–4982. (b) Foster, E. J.; Berda, E. B.; Meijer, E. W. Metastable Supramolecular Polymer Nanoparticles via Intramolecular Collapse of Single Polymer Chains. *J. Am. Chem. Soc.* **2009**, *131*, 6964–6966. (c) Ogi, S.; Sugiyasu, K.; Manna, S.; Samitsu, S.; Takeuchi, M. Living Supramolecular Polymerization Realized through a Biomimetic Approach. *Nat. Chem.* **2014**, *6*, 188–195. (d) Kang, J.; Miyajima, D.; Mori, T.; Inoue, Y.; Itoh, Y.; Aida, T. A Rational Strategy for the Realization of Chain-Growth Supramolecular Polymerization. *Science* **2015**, *347*, 646–651. (e) Ogi, S.; Stepanenko, V.; Sugiyasu, K.; Takeuchi, M.; Würthner, F. Mechanism of Self-Assembly Process and Seeded Supramolecular Polymerization of Perylene Bisimide Organogelator. *J. Am. Chem. Soc.* **2015**, *137*, 3300–3307. (f) Greciano, E. E.; Sánchez, L. Seeded Supramolecular Polymerization in a Three-Domain Self-Assembly of an N-Annulated Perylenetetracarboxamide. *Chem. - Eur. J.* **2016**, *22*, 13724–13730.

(23) (a) Ikai, T.; Takagi, Y.; Shinohara, K.; Maeda, K.; Kanoh, S. Synthesis of Polyisocyanides Bearing Oligothiophene Pendants: Higher-Order Structural Control through Pendant Framework Design. *Polym. J.* **2015**, *47*, 625–630. (b) Ikai, T.; Wada, Y.; Takagi, Y.; Shinohara, K. Impact of a Minority Enantiomer on the Polymerization of Alanine-Based Isocyanides with an Oligothiophene Pendant. *Polym. Chem.* **2016**, *7*, 7057–7067.

(24) We also confirmed that no Cotton effect appeared over the entire absorption region of *supra*-poly(**3**).

(25) In fact, the absorption spectral pattern of *supra*-poly(**3**$_{1-r}$-*co*-**2L**$_r$) was almost identical to that of the **2L** monomer (Figure S14A), suggesting that the absorption derived from the BDT pendant units covered the entire area from the absorption onset of ca. 460 nm to the lowest wavelength employed (235 nm).

(26) Takei, F.; Onitsuka, K.; Takahashi, S.; Terao, K.; Sato, T. Control of Helical Structure in Random Copolymers of Chiral and Achiral Aryl Isocyanides Prepared with Palladium–Platinum μ-Ethynediyl Complexes. *Macromolecules* **2007**, *40*, 5245–5254.

(27) We recently reported a cellulose-based static helical polymer with similar BDT pendant groups.[19] In that case, the CD intensity derived from the BDT units greatly changed depending on their chiral arrangement along the helical backbone, with more than tenfold variation was observed.

(28) The influence of optical anisotropy on the films used in this study was confirmed to be almost negligible (Figure S23).

(29) (a) Chan, C. Y. K.; Lam, J. W. Y.; Deng, C.; Chen, X.; Wong, K. S.; Tang, B. Z. Synthesis, Light Emission, Explosive Detection, Fluorescent Photopatterning, and Optical Limiting of Disubstituted Polyacetylenes Carrying Tetraphenylethene Luminogens. *Macromolecules* **2015**, *48*, 1038–1047. (b) He, Y.-G.; Shi, S.-Y.; Liu, N.; Ding, Y.-S.; Yin, J.; Wu, Z.-Q. Tetraphenylethene-Functionalized Conjugated Helical Poly(phenyl isocyanide) with Tunable Light Emission, Assembly Morphology, and Specific Applications. *Macromolecules* **2016**, *49*, 48–58.

Authors are required to submit a graphic entry for the Table of Contents (TOC) that, in conjunction with the manuscript title, should give the reader a representative idea of one of the following: A key structure, reaction, equation, concept, or theorem, etc., that is discussed in the manuscript. Consult the journal's Instructions for Authors for TOC graphic specifications.

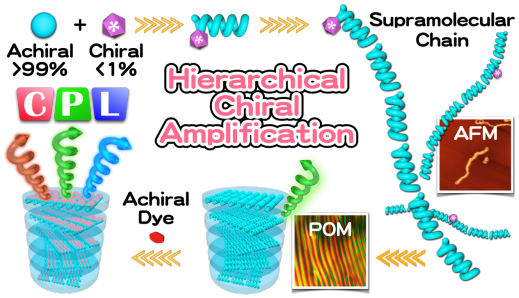

Insert Table of Contents artwork here